

Phase partitioning and site-preference of hafnium in the $\gamma'(L1_2)/\gamma(\text{fcc})$ system in Ni-based superalloys: An atom-probe tomographic and first-principles study

Yaron Amouyal,^{1,a)} Zungang Mao,^{1,b)} and David N. Seidman^{1,2,c)}

¹Department of Materials Science and Engineering, Northwestern University, 2220 Campus Drive, Evanston, Illinois 60208-3108, USA

²Northwestern University Center for Atom-Probe Tomography (NUCAPT), 2220 Campus Drive, Evanston, Illinois 60208-3108, USA

(Received 12 August 2009; accepted 16 September 2009; published online 22 October 2009)

Atom-probe tomography (APT) and first-principles calculations are employed to investigate the partitioning of Hf in the $\gamma'(L1_2)/\gamma(\text{fcc})$ phases in two multicomponent Ni-based superalloys. APT results indicate strong partitioning of Hf atoms to the $\gamma(\text{fcc})$ -phase. We perform first-principles calculations of the substitutional formation energy of Hf for a model $\gamma(\text{Ni})/\gamma'(\text{Ni}_3\text{Al})$ system indicating Hf partitioning to the γ' -phase. Additional calculations of the Hf–Cr binding energy suggest, however, that Cr atoms, which partition to the γ -phase, have a strong attractive binding energy with Hf atoms, thus predicting a reversal of the Hf partitioning in favor of the γ -phase due to alloying with Cr. © 2009 American Institute of Physics. [doi:10.1063/1.3248146]

Nickel-based superalloys are utilized for turbine blades in aeronautical jet engines and land-based power generators owing to their excellent high-temperature strength and creep rupture resistance. These mechanical properties are associated with their unique microstructure comprising Ni₃Al-based $\gamma'(L1_2)$ -precipitates dispersed in a Ni-based $\gamma(\text{fcc})$ -matrix.^{1,2} Hafnium is added to Ni-based superalloys in small concentrations (0.05–0.5 at. %) to increase the transverse ductility of the directionally solidified turbine blades by strengthening their grain boundaries,¹ as well as to improve the adherence of the protective oxide layer.³ The question of whether Hf partitions to the γ - or γ' -phases is technologically important since Hf can strongly affect the lattice parameter misfit due to its large atomic radius.^{2,4} Moreover, Hf can play an important role modifying the density of the liquid during solidification, causing the formation of misoriented grains,^{5,6} which is associated with γ/γ' partitioning.

In spite of these important implications, very little is known about the γ/γ' partitioning behavior of Hf. Calculated equilibrium phase diagrams of the ternary Ni–Al–Hf system predict partitioning of Hf to the γ' -phase,⁷ and a similar trend occurs in a few experimental studies of multicomponent Ni-based alloys.^{8–10} There are, however, some exceptions,² which can be attributed to alloy composition, since the partitioning behavior of minority elements can be changed as a result of their interactions with other elements and, in specific cases, can even be reversed.¹¹ An investigation of the partitioning behavior of Hf in other multicomponent Ni-based alloys, combining both experimental and theoretical approaches will enable us to understand its dependence on alloy composition. We present an atom-probe tomographic (APT) study of the partitioning behavior of Hf to the γ - and γ' -phases in two multicomponent Ni-based

alloys, which is combined with first-principles calculations of the substitutional formation energies of Hf and Cr at different sublattice sites in a model γ/γ' system. We hypothesize that Cr has a major effect on the partitioning behavior of Hf, which is further corroborated by calculating Hf–Cr binding energies in the γ - and γ' -phases.

Two multicomponent Ni-based superalloys were directionally solidified along the $\langle 100 \rangle$ -orientation employing the Bridgman technique.² The first alloy, ME-9, has the nominal composition Ni–14.6 Al–8.18 Cr–7.74 Co–1.95 Ta–0.95 Mo–2.31 W–1.47 Re–0.63 C–0.05 Hf at. %, and the second, ME-15, has the composition Ni–15.1 Al–7.73 Cr–7.31 Co–1.97 Ta–0.9 Mo–0.75 W–0.46 Re–0.67 C–0.05 Hf at. %.⁶ APT specimens were prepared from the as-solidified samples by electropolishing and analyzed using pulsed-laser local-electrode atom probe (LEAP) tomography.^{12,13} Experimental conditions are described elsewhere.¹¹

A typical three-dimensional APT reconstruction taken from ME-15, exhibiting both γ - and γ' -phases, is displayed in Fig. 1(a). For clarity, only the Al, Cr, and Hf atoms are displayed, indicating the predominance of Al (red) in the γ' -phase and Cr (blue) in the γ -phase. Pronounced partitioning of Hf (represented as large black spheres) to the γ -phase is also observed. The partitioning of Hf between the phases is quantitatively displayed in the proxigram,¹¹ Fig. 1(b), with a partitioning ratio $K_{\text{Hf}}^{\gamma'/\gamma} = 0.157 \pm 0.024$, where $K_i^{\gamma'/\gamma}$ is defined as the ratio of the concentration of an element i in the γ' -phase to its concentration in the γ -phase.¹¹ For comparison, the proxigrams of Al and Cr are exhibited in Fig. 1(b).

Similar values of $K_{\text{Hf}}^{\gamma'/\gamma} = 0.142 \pm 0.017$ were measured for ME-9, indicating that Hf prefers partitioning to the γ -phase. All the other elements exhibit the standard partitioning behavior typical for Ni-based superalloys.¹¹ Our results disagree with prior APT studies, which indicate that Hf partitions to the γ' -phase ($K_{\text{Hf}}^{\gamma'/\gamma} > 1$).^{8–10} This difference is attributed to the alloys' compositions. Among the major alloying elements, Cr is known to play a significant role in stabilizing the γ -phase, which results in increasing the solu-

^{a)}Electronic mail: y-amouyal@northwestern.edu.

^{b)}Electronic mail: z-mao2@northwestern.edu.

^{c)}Author to whom correspondence should be addressed. Electronic mail: d-seidman@northwestern.edu. Tel.: +1-847-491-4391.

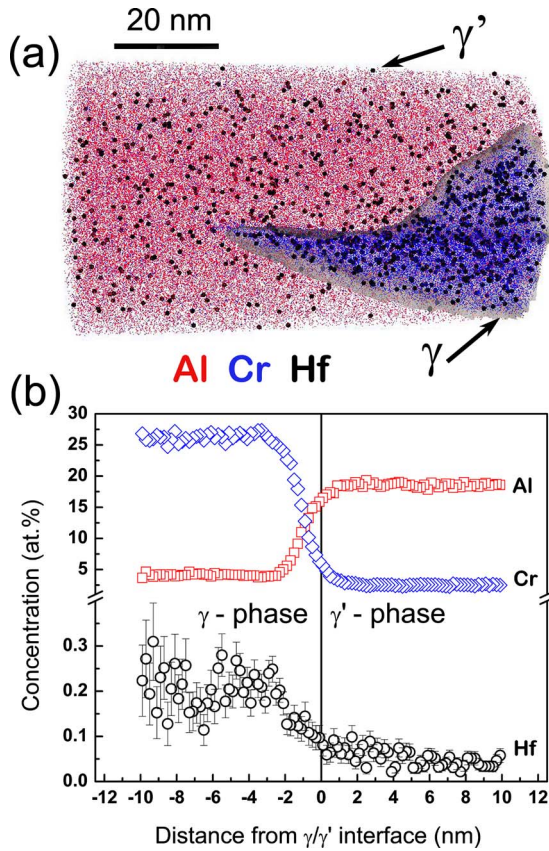


FIG. 1. (Color online) (a) A 3D-APT reconstruction showing the γ (fcc)- and γ' (L_{12})-phases in ME-15. The phases are separated by a 5.9 at. % Cr iso-concentration surface. Only 15% of the Al (red), 15% of the Cr (blue), and 80% of the Hf (large spheres) atoms are shown for clarity. (b) The concentrations of Al, Cr, and Hf are plotted as a function of distance from the γ/γ' interface, which demonstrates that the γ -phase has a strong preference for Hf.

bilities of elements in it.¹ Thus, we hypothesize that the $K_{\text{Hf}}^{\gamma'/\gamma}$ -values will decrease due to alloying with Cr and may be ultimately reversed to values < 1 .

To understand the γ/γ' partitioning of Hf and the effect of Cr on it, we performed first-principles calculations of the substitutional formation energies of Hf and Cr in two model Hf- or Cr-microalloyed Ni–Al systems at 0 K, respectively. The system simulated is a supercell of $16 \times 2 \times 2$ - points divided into two halves: a Ni–fcc lattice (γ -phase) and a Ni_3Al lattice having the L_{12} structure (γ' -phase) separated by a $\{100\}$ interface. We applied the general gradient approximation with an energy cutoff of 300 eV in the Vienna *ab initio* simulation package (VASP).^{14,15} A more detailed description of the simulation procedure can be found elsewhere.^{11,16} The substitutional formation energies of Hf or Cr were calculated by placing Hf or Cr at different sites close to the $\{100\}$ γ/γ' interfaces.¹⁶ The calculations are performed using the following relationships:

$$E_{M \rightarrow \text{Ni}}^{\gamma} \equiv [(E_{M \text{ in } \gamma}^{\text{tot}} + n_{\text{Ni}}\mu_{\text{Ni}}) - (E^{\text{tot}} + n_M\mu_M)]/n_M \quad (1)$$

for M substituting for Ni in the γ -phase, and

$$E_{M \rightarrow \text{Ni or Al}}^{\gamma'} \equiv [(E_{M \text{ in } \gamma'}^{\text{tot}} + n_{\text{Ni or Al}}\mu_{\text{Ni or Al}}) - (E^{\text{tot}} + n_M\mu_M)]/n_M \quad (2)$$

for M substituting for Ni or Al in the γ' -phase, where M represents the substituting atom, either Hf or Cr, and E^{tot} is

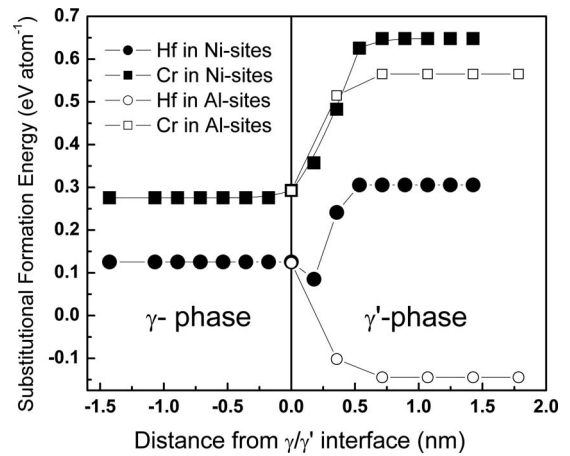


FIG. 2. The substitutional formation energies of Hf (circles) and Cr (squares) atoms in Ni- (solid symbols) and Al- (open symbols) sublattice sites as a function of their distances from the $\{100\}$ γ/γ' interface, obtained using first-principles calculations performed for a model $\text{Ni}(\gamma)/\text{Ni}_3\text{Al}(\gamma')$ system. The preferences of Hf for the Al-sites of the γ' -phase and of Cr for the γ -phase are thereby demonstrated.

the total energy of the supercell, including the interface, prior to substitution. E_M^{tot} in γ' and E_M^{tot} in γ are the total energies of the M -microalloyed supercell, containing the interface, calculated for substitution in the γ' - or γ -phases, respectively. μ_i is the chemical potential of the i th atom calculated assuming the same cell symmetry. Figure 2 displays the substitutional formation energies of Hf and Cr as a function of their distances from the $\{100\}$ interface. Fig 2 indicates that Hf prefers partitioning to the γ' -phase,⁷ while Cr prefers the γ -phase.¹⁷ Both Hf and Cr prefer the Al-sublattice sites of the γ' -phase. The driving force for γ' -partitioning,¹¹ defined as $E_{M \rightarrow \text{Al}}^{\gamma'} - E_{M \rightarrow \text{Ni}}^{\gamma}$, is $0.270 \text{ eV atom}^{-1}$ for Hf and $-0.290 \text{ eV atom}^{-1}$ for Cr.

In addition to the above, we employ the first-principles approach to calculate the binding energies between Hf and Cr atoms in both the γ - and γ' -phases, at 0 K, to determine how the Cr atoms affect the phase or site preference of Hf atoms. We define the binding energy between two solute atoms as the difference between two terms: the first one (the *interaction term*) is the total energy of a cell containing a Hf–Cr dimer, and the second one (the *reference term*) is the sum of the total energies of two subcells containing one solute atom each. To calculate the interaction term, we constructed a model γ -Ni phase consisting of $4 \times 2 \times 2$ fcc unit cells (64 atoms). Hf and Cr atoms were placed at different interatomic separations from each other, ranging from the first to the tenth nearest-neighbor (NN) distance, and the total energy of this γ -cell, $E_{i,\gamma}^{\text{Hf+Cr}}$, was calculated. For the reference term, we construct two $2 \times 2 \times 2$ fcc unit cells of γ -Ni, each containing 32 atoms. Then, we placed one Hf atom substituting for a Ni atom in one cell and calculated its total energy, $E_{\gamma}^{\text{Hf} \rightarrow \text{Ni}}$. The same calculation was performed for a Cr atom in the second cell, having a total energy of $E_{\gamma}^{\text{Cr} \rightarrow \text{Ni}}$. From this definition, the binding energy of a Hf–Cr dimer for an i th NN position in the $\gamma(\text{Ni})$ -phase ($E_{i,\gamma}^b$) is given by the following definition:

$$E_{i,\gamma}^b \equiv E_{i,\gamma}^{\text{Hf+Cr}} - (E_{\gamma}^{\text{Hf} \rightarrow \text{Ni}} + E_{\gamma}^{\text{Cr} \rightarrow \text{Ni}}). \quad (3)$$

A similar procedure is performed for the model γ' - Ni_3Al phase. In this case, the total energies depend on the positions of the solute atoms at the Ni- or Al-sublattice sites. To cal-

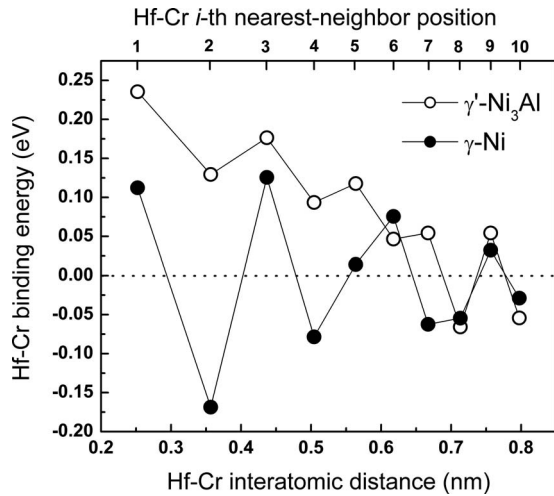


FIG. 3. The Hf–Cr binding energies (eV), for Hf–Cr dimers, in the Ni(γ - and Ni₃Al(γ')-phases as a function of the interatomic distance (nm) ranging from the first through the tenth NN distances. The Hf–Cr binding energy is repulsive for the γ' -phase (open circles) through the seventh NN distance, and is attractive for the γ -phase (solid circles) for the second, fourth, seventh, eighth, and tenth NN distances.

culate the interaction term, the Hf atom is fixed in the Al sublattice, due to its lower (negative) substitutional formation energy, $E_{\text{Hf} \rightarrow \text{Al}}^{\gamma'} = -0.144 \text{ eV atom}^{-1}$, as opposed to Cr with a higher (positive) value of $E_{\text{Cr} \rightarrow \text{Al}}^{\gamma'} = 0.565 \text{ eV atom}^{-1}$, Fig. 2. Next, the Cr atom is placed at an i th NN position (either Ni- or Al-sublattice site) with respect to the Hf atom, and the total energy of the cell, $E_{i,\gamma'}^{\text{Hf+Cr}}$, is calculated. The calculation of the total energy of the Hf-containing cell, $E_{\gamma'}^{\text{Hf} \rightarrow \text{Al}}$, in the reference term is performed similarly to the one for the γ -Ni phase, where the Hf atom is placed in an Al site only. For the Cr-containing cell, however, the Cr atom is placed in one of the two possible sites: a Ni- or an Al-sublattice site, depending on the value of i , and the total energy, $E_{i,\gamma'}^{\text{Cr} \rightarrow \text{Ni or Al}}$, is then calculated. The binding energy of a Hf–Cr dimer for the i th NN position in the γ' -Ni₃Al phase, $E_{i,\gamma'}^b$, is given by the following definition:

$$E_{i,\gamma'}^b \equiv E_{i,\gamma'}^{\text{Hf+Cr}} - (E_{\gamma'}^{\text{Hf} \rightarrow \text{Al}} + E_{i,\gamma'}^{\text{Cr} \rightarrow \text{Ni or Al}}). \quad (4)$$

For the defined binding energies, Eqs. (3) and (4), a positive value, $E_i^b > 0$, is repulsive and a negative value, $E_i^b < 0$, is attractive. Figure 3 displays the binding energies as a function of the Hf–Cr interatomic distance for both phases.

Figure 3 shows that $E_{i,\gamma'}^b > 0$ up to $i=7$ for the γ' -phase, meaning that the Cr–Hf interaction is repulsive with the value of $E_{1,\gamma'}^b = 0.236$ and $E_{7,\gamma'}^b = 0.054 \text{ eV}$ at the first and seventh NN distances, respectively. The repulsive values of $E_{i,\gamma'}^b$ decrease with increasing Hf–Cr separation through $i=7$, with local minima at the second, fourth, and sixth (i even) NN positions, and then $E_{i,\gamma'}^b$ fluctuates about $E_{i,\gamma'}^b = 0$ with attractive values for $i=8$ and 10 , and a repulsive value for $i=9$. In the γ -phase, importantly, there is an attractive interaction, $E_{i,\gamma}^b < 0$, between Cr and Hf when located at the second, fourth, seventh, eighth, and tenth NN positions. These attractive interactions are $E_{2,\gamma}^b = -0.169$ and $E_{7,\gamma}^b = -0.062 \text{ eV}$ at the second and seventh NN positions, respectively. It follows that the Cr atoms, which prefer the

γ -phase, Fig. 2, bind strongly with Hf atoms at interatomic separation as small as the second NN positions, attracting them into the γ -phase. Furthermore, the binding energy of Cr–Hf dimers in the γ' -phase is repulsive for a wide range of interatomic separations up to the eighth NN position, implying that the presence of Cr in the γ' -phase rejects Hf atoms into the γ -phase. We, therefore, anticipate that Cr atoms will change the partitioning behavior of Hf in favor of the γ -phase, decreasing $K_{\text{Hf}}^{\gamma'/\gamma}$ values to less than unity. This also explains the difference between our APT results and other results,^{7–10} because the concentration of Cr in our samples is relatively large.

In summary, APT measurements of the compositions of the γ - and γ' -phases in two multicomponent Ni-based alloys indicate that Hf partitions strongly to the γ -phase. Conversely, first-principles calculations of the substitutional formation energy of Hf in a model Ni(fcc)/Ni₃Al(L1₂) system predict, with this as a sole criterion, that Hf partitions to the γ' -phase. Applying a first-principles approach for calculating the binding energies between Hf and Cr atoms, we demonstrate that Cr can reverse the γ' -preference of Hf in favor of the γ -phase, which can result in $K_{\text{Hf}}^{\gamma'/\gamma} < 1$ values. We conclude that the concentration of Cr influences the γ/γ' partitioning and needs to be accounted for in the design of Ni-based superalloys.

The research was supported by MEANS II AFOSR Grant No. FA9550-05-1-0089. We acknowledge partial support from the National Science Foundation (DMR-0804610) for Z.M. and from the Marie Curie IOF (CEC FP7) for Y.A. Dr. L. Graham and Prof. T. Pollock are kindly thanked for supplying alloys. The LEAP tomograph was purchased with funding from the NSF-MRI and ONR-DURIP programs. The authors acknowledge Dr. C. Booth-Morrison for helpful discussions and Dr. D. Isheim for managing NUCAPT.

¹M. Durand-Charre, *The Microstructure of Superalloys* (Gordon and Breach Science, Amsterdam, 1997).

²R. C. Reed, *The Superalloys: Fundamentals and Applications* (Cambridge University Press, New York, 2006).

³J. L. Smialek and G. N. Morscher, *Mater. Sci. Eng., A* **332**, 11 (2002).

⁴D. Blavette, E. Cadel, C. Pareige, B. Deconihout, and P. Caron, *Microsc. Microanal.* **13**, 464 (2007).

⁵S. M. Roper, S. H. Davis, and P. W. Voorhees, *J. Fluid Mech.* **596**, 333 (2008).

⁶S. Tin and T. M. Pollock, *J. Mater. Sci.* **39**, 7199 (2004).

⁷C. Zhang, J. Zhu, Y. Yang, H. B. Cao, F. Zhang, W. S. Cao, and Y. A. Chang, *Intermetallics* **16**, 139 (2008).

⁸R. C. Reed, A. C. Yeh, S. Tin, S. S. Babu, and M. K. Miller, *Scr. Mater.* **51**, 327 (2004).

⁹K. E. Yoon, D. Isheim, R. D. Noebe, and D. N. Seidman, *Interface Sci.* **9**, 249 (2001).

¹⁰H. Murakami, H. Harada, and H. K. D. H. Bhadeshia, *Appl. Surf. Sci.* **76**, 177 (1994).

¹¹Y. Amouyal, Z. Mao, C. Booth-Morrison, and D. N. Seidman, *Appl. Phys. Lett.* **94**, 041917 (2009).

¹²D. N. Seidman, *Annu. Rev. Mater. Res.* **37**, 127 (2007).

¹³T. F. Kelly and M. K. Miller, *Rev. Sci. Instrum.* **78**, 031101 (2007).

¹⁴G. Kresse and J. Furthmüller, *Phys. Rev. B* **54**, 11169 (1996).

¹⁵G. Kresse and J. Hafner, *Phys. Rev. B* **49**, 14251 (1994).

¹⁶Y. Amouyal, Z. Mao, and D. N. Seidman, *Appl. Phys. Lett.* **93**, 201905 (2008).

¹⁷C. Booth-Morrison, Z. Mao, R. D. Noebe, and D. N. Seidman, *Appl. Phys. Lett.* **93**, 033103 (2008).